Inorganic Chemistry
Article

Inorg. Chem. **2009**, *48*, 8037–8043 **8037**
DOI: 10.1021/ic9007153

Synthesis, Structure, and Reactivity of Low-Coordinate 1,1,3,3-Tetraethylguanidinate Complexes

Scott D. Bunge,* Jeffrey A. Bertke, and Travis L. Cleland

Kent State University, Department of Chemistry, Kent, Ohio 44242

Received April 13, 2009

Diethylcyanamide is added to a hexanes solution of lithium diethylamide [$LiN(CH_2CH_3)_2$] resulting in the formation of lithium 1,1,3,3-tetraethylguanidinate, [Li(μ-TEG)]$_6$ (**1**). Upon successful isolation of **1**, the metathesis reaction of MX_2 (MX_2 = $MnBr_2$, $FeBr_2$, $CoBr_2$, and $ZnCl_2$) with [Li(μ-TEG)]$_6$ and lithium bistrimethylsilylamide, $LiN(SiMe_3)_2$, was performed to generate dinuclear tetraethylguanidinate (TEG) complexes with the general formula [M(μ-TEG)-{$N(SiMe_3)_2$}]$_2$ {M = Mn (**2**), Fe (**3**), Co (**4**), Zn (**5**)}. Further reaction of **2** with 2 equiv of ethanol (EtOH) and 2 equiv of 2,6-ditert-butylphenol (H-DBP) results in the formation of the manganese alkoxide, [Mn(μ-OEt)(DBP)(H-TEG)]$_2$ (**6**). Elemental analysis, FT-IR spectroscopy, UV−vis spectroscopy, and single crystal X-ray diffraction were utilized to characterize the six compounds.

Introduction

N-substituted guanidinate anions (see Chart 1, L^1 and L^2) have received increasing attention within the past fifteen years as ancillary ligands for main-group, *d*-block, and lanthanide complexes.[1] This is due in part to the guanidinate's flexible coordination behavior and its tunable steric and electronic properties. A characteristic feature of these ligands is the presence of a Y-shaped "CN_3" core that is capable of shuttling electron density.[2] This resonance provides the possibility for strong coordination of the N-donors to metals possessing a range of Lewis acidity. As a result, L^1 and L^2 have proven to be useful ligands for homogeneous catalysts, metal−metal bonding studies, and metal facilitated small molecule activation.[3] In a testament to the guanidinate's versatility, the bicyclic L^2 ligand has been shown to be an effective N-donor for the isolation of remarkably stable gold(I) and gold(II) complexes.[4]

In contrast to the variety of complexes found with L^1 and L^2, the coordination chemistry of the monoanioinc 1,1,3,3-tetraalkylguanidinate (TAG) derivative (see Chart 1, L^3) has received far less notice.[2] In the 1960s, a pioneering study on reactions of organolithium compounds with 1,1,3,3-tetramethylguanidine (H-TMG) was reported by Wade and co-workers.[5−7] In this and subsequent investigations, the guanidine was deprotonated via an organolithium reagent to generate [Li(μ-TMG)]$_6$. Alternatively, 1 equiv of lithium dimethlyamide was stated to react with dimethylcyanamide to also cleanly generate the lithium guanindinate. Notably, additional investigations extending this work have been limited and typically utilize the commercially available TMG.[8−10]

*To whom correspondence should be addressed. E-mail: sbunge@kent.edu. Phone: (330)672-9445.

(1) For reviews related to guanidinate coordination chemistry see: Edelmann, F. T. *Adv. Organomet. Chem.* **2008**, *57*, 183. Coles, M. P. *Dalton Trans.* **2006**, 985. Bailey, P. J.; Pace, S. *Coord. Chem. Rev.* **2001**, *214*, 91.

(2) Gobbi, A.; Frenking, G. *J. Am. Chem. Soc.* **1993**, *115*, 2362.

(3) For selected examples see: Duncan, A. P.; Mullins, S. M.; Arnold, J.; Bergman, R. G. *Organometallics* **2001**, *20*, 1808. Lyubov, D. M.; Bubnov, A. M.; Fukin, G. K.; Dolgushin, F. M.; Antipin, M. Y.; Pelce, O.; Schappacher, M.; Guillaume, S. M.; Trifonov, A. A. *Eur. J. Inorg. Chem.* **2008**, 2090. Cotton, F. A.; Daniels, L. M.; Murillo, C. A.; Timmons, D. J.; Wilkinson, C. C. *J. Am. Chem. Soc.* **2002**, *124*, 9249. Cotton, F. A.; Gruhn, N. E.; Gu, J.; Huang, P.; Lichtenberger, D. L.; Murillo, C. A.; Van Dorn, L. O.; Wilkinson, C. C. *Science* **2002**, *298*, 1971. Cotton, F. A.; Donahue, J. P.; Lichtenberger, D. L.; Murillo, C. A.; Villagran, D. *J. Am. Chem. Soc.* **2005**, *127*, 10808. Cotton, F. A.; Huang, P.; Murillo, C. A.; Timmons, D. J. *Inorg. Chem. Commun.* **2002**, *5*, 501. Berry, J. F.; Cotton, F. A.; Huang, P.; Murillo, C. A.; Wang, X. *Dalton Trans.* **2005**, 3713.

(4) Mohamed, A. A.; Mayer, A. P.; Abdou, H. E.; Irwin, M. D.; Perez, L. M.; Fackler, J. P., Jr. *Inorg. Chem.* **2007**, *46*, 11165.

(5) Pattison, I.; Wade, K.; Wyatt, B. K. *J. Chem. Soc., A* **1968**, 837. Barnett, N. D. R.; Mulvey, R. E.; Clegg, W.; Oneil, P. A. *Polyhedron* **1992**, *11*, 2809.

(6) Clegg, W.; Mulvey, R. E.; Snaith, R.; Toogood, G. E.; Wade, K. *J. Chem. Soc., Chem. Commun.* **1986**, 1740.

(7) Armstrong, D. R.; Barr, D.; Snaith, R.; Clegg, W.; Mulvey, R. E.; Wade, K.; Reed, D. *J. Chem. Soc., Dalton Trans.* **1987**, 1071.

(8) Stalke, D.; Paver, M. A.; Wright, D. S. *Angew. Chem., Int. Ed. Engl.* **1993**, *32*, 428.

(9) Peters, K.; Peters, E. M.; von Schnering, H. G.; Schmidt, A. *Z. Kristallogr.* **1993**, *205*, 279. Edwards, A. J.; Paver, M. A.; Raithby, P. R.; Rennie, M. A.; Russell, C. A.; Wright, D. S. *J. Chem. Soc., Dalton Trans.* **1995**, 1587. Kretschmer, W. P.; Dijkhuis, C.; Meetsma, A.; Hessen, B.; Teuben, J. H. *Chem. Commun.* **2002**, 608. Cowley, A. R.; Downs, A. J.; Himmel, H. J.; Marchant, S.; Parsons, S.; Yeoman, J. A. *Dalton Trans.* **2005**, 1591. Zhang, J.; Zhou, X.; Cai, R.; Weng, L. *Inorg. Chem.* **2005**, *44*, 716. Rische, D.; Baunemann, A.; Winter, M.; Fischer, R. A. *Inorg. Chem.* **2006**, *45*, 269. Milanov, A.; Bhakta, R.; Baunemann, A.; Becker, H.-W.; Thomas, R.; Ehrhart, P.; Winter, M.; Devi, A. *Inorg. Chem.* **2006**, *45*, 11008. Dornan, P.; Rowley, C. N.; Priem, J.; Barry, S. T.; Burchell, T. J.; Woo, T. K.; Richeson, D. S. *Chem. Commun.* **2008**, 3645.

(10) Bunge, S. D.; Lance, J. M.; Bertke, J. A. *Organometallics* **2007**, *26*, 6320.

Published on Web 07/22/2009

Chart 1. Structures of Monoanionic Guanidinate Ligands[a]

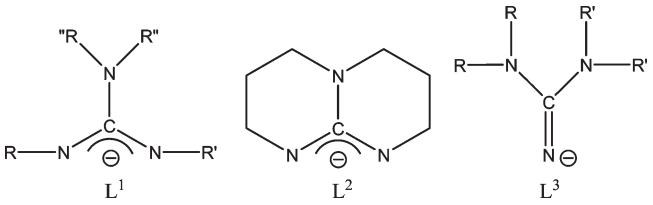

[a] R, R′ and R″ = silyl, alkyl or aryl.

Because of the versatility of the TAG framework, our research group has initiated an effort to further detail the coordination chemistry and reactivity.[11−13] We envisioned that utilizing bulky TAG ligands in conjunction with $[N(SiMe_3)_2]$ would facilitate the isolation of well-defined low-coordinate complexes. The resulting coordinatively unsaturated systems could then be readily reacted with protic reagents such as alcohols, thiols, and primary amines to generate reagents for areas such as nanocrystal synthesis and chemical vapor deposition.[14] Toward this goal, the synthesis of lithium 1,1,3,3-tetraethylguanidinate $[Li(\mu\text{-TEG})]_6$ (**1**) is described herein, and its use for the isolation of a family of *d*-block metal complexes with the general formula $[M(\mu\text{-TEG})\{N(SiMe_3)_2\}]_2$ {M = Mn (**2**), Fe (**3**), Co (**4**), and Zn (**5**)} reported. The reactivity of **2** was further investigated through reaction with $HOC_6H_3(CMe_3)_2$-2,6 (H-DBP) and ethanol (H-OEt) in a 1:2 ratio to form the resultant $[Mn(\mu\text{-OEt})(DBP)(H\text{-TEG})]_2$ (**6**). The six novel compounds were characterized by single-crystal X-ray diffraction. The bulk powders for all complexes were found to be in agreement with the crystal structures based on elemental analyses, FT-IR spectroscopy, ^1H and ^{13}C NMR studies.

Experimental Section

All syntheses were handled with rigorous exclusion of air and water using standard glovebox techniques. All anhydrous solvents were stored under argon and used as received in sure seal bottles. The following chemicals were used as received from commercial suppliers: $LiN(CH_2CH_3)_2$, diethylcyanamide, $LiN(SiMe_3)_2$, $ZnCl_2$, $MnBr_2$, $FeBr_2$, and $CoBr_2$. FT-IR data were obtained on a Bruker Tensor 27 Instrument using a KBr window under an atmosphere of flowing nitrogen. Electronic absorption spectra were obtained on a Cary 5000 UV−vis spectrophotometer. Elemental analysis was performed on a Perkin-Elmer 2400 Series 2 CHN-S/O Elemental Analyzer. Magnetic susceptibility measurements for **2**−**4** and **6** were measured at 298 K and determined in solution by the method of Evans.[15] The calculated magnetic moments were corrected for underlying diamagnetism. All NMR samples were prepared from dried crystalline materials that were handled and stored under an argon atmosphere and redissolved in toluene-d_8. All solution spectra were obtained on a Bruker DRX 400 spectrometer at 400.1 and 100.6 MHz for ^1H and ^{13}C experiments.

Synthesis of $[Li(\mu\text{-TEG})]_6$ (1). A hexanes solution of diethylcyanamide (0.31 g, 3.0 mmol) (5 mL) was added dropwise to a hexanes solution (10 mL) of $LiN(CH_2CH_3)_2$ (0.25 g, 3.0 mmol). The solution was heated to reflux for 10 min and then allowed to evaporate yielding colorless crystals within 12 h. Yield 78% (0.44 g, 2.3 mmol). ^1H NMR (toluene-d_8): δ 3.14 (m, 8 H, N=C(N(CH_2CH_3)$_2$)$_2$), 1.10 (m, 12 H, N=C(N(CH_2CH_3)$_2$)$_2$). ^{13}C NMR (toluene-d_8): δ 154.6(N=*C*(N(CH_2CH_3)$_2$)$_2$), 42.7 (N=C(N(*C*H_2CH_3)$_2$)$_2$),14.4 (N=C(N(CH_2CH_3)$_2$)$_2$). FT-IR (KBr, cm^{-1}) 2966 (s), 2895 (s), 1545 (s), 1459 (m), 1405 (m), 1380 (m), 1245 (m), 1119 (w), 1077 (w), 1006 (m), 938 (w), 879 (m), 842 (m), 749 (w), 669 (w), 633 (w), 612 (w), 561 (w), 482 (w).

General Synthesis of 2−5. Lithium diethylamide (0.237 g, 3 mmol) was dissolved in ether (10 mL). To this solution, diethylcyanamide (0.294 g, 3 mmol), dissolved in ether (5 mL), was added dropwise and allowed to stir for approximately 15 min. $LiN(SiMe_3)_2$ (0.501 g, 3 mmol) was subsequently dissolved in the solution. MBr_2 (M = Mn, Fe, Co) or $ZnCl_2$ (3 mmol) was then added, and the reaction stirred for 24 h. The volatiles were then removed under vacuum, and the remaining solid was dissolved in hexanes. The solution was then centrifuged, the liquid was decanted off, concentrated, and placed in a −35 °C freezer. Crystals {pink (**2**), yellow (**3**), blue (**4**), colorless (**5**)} formed within 24 h.

$[Mn(\mu\text{-TEG})\{N(SiMe_3)_2\}]_2$ (2). Yield 25% (0.30 g, 0.38 mmol). Anal. Calcd for $C_{30}H_{76}Mn_2N_8Si_4$: C 46.72, H 9.93, N 14.53. Found: C 47.19, H 10.17, N 14.12. FT-IR (KBr, cm^{-1}) 2972 (s), 2945 (s), 2894 (m), 2875 (m), 1528 (s), 1509 (s), 1463 (s), 1377 (m), 1250 (s), 1211 (w), 1191 (w), 1121 (m), 1072 (m), 1012 (s), 937 (m), 874 (s), 827 (s), 778 (m), 666 (m), 612 (m). UV−vis absorption spectra λ_{max} (nm) and ε (mL mol^{-1} cm^{-1}) values in parentheses: 328 (36700). Magnetic moment (μ_B): 4.30.

$[Fe(\mu\text{-TEG})\{N(SiMe_3)_2\}]_2$ (3). Yield 45% (0.52 g, 0.68 mmol). Anal. Calcd for $C_{30}H_{76}Fe_2N_8Si_4$: C 46.61, H 9.91, N 14.50. Found: C 45.88, H 9.54, N 15.42. FT-IR (KBr, cm^{-1}) 2948 (m), 2895 (w), 1514 (s), 1455 (s), 1438 (s), 1409 (w), 1378 (m), 1345 (s), 1261 (s), 1240 (s), 1126 (w), 1056 (w), 978 (s), 944 (m), 868 (s), 847 (s), 788 (m), 750 (w), 669 (m), 612 (w), 573 (w). UV−vis absorption spectra (nm) and ε (mL mol^{-1} cm^{-1}) values in parentheses: 301 (128000), 388 (14800), 456 (6710). Magnetic moment (μ_B) 2.77.

$[Co(\mu\text{-TEG})\{N(SiMe_3)_2\}]_2$ (4). Yield 66% (0.77 g, 1.0 mmol). Anal. Calcd for $C_{30}H_{76}Co_2N_8Si_4$: C 46.24, H 9.83, N 14.38. Found: C 45.90, H 9.14, N 14.72. FT-IR (KBr, cm^{-1}) 2966 (s), 2896 (m), 1535 (s), 1460 (s), 1399 (m), 1377 (m), 1355 (m), 1255 (s), 1243 (s), 1214 (w), 1198 (w), 1123 (m), 1073 (m), 1051 (m), 998 (s), 938 (m), 867 (s), 843 (s), 827 (s), 785 (m), 749 (m), 668 (m). UV−vis absorption spectra λ_{max} (nm) and ε (mL mol^{-1} cm^{-1}) values in parentheses: 279 (289000), 504 (28500), 688 (13900). Magnetic moment (μ_B): 3.35.

$[Zn(\mu\text{-TEG})\{N(SiMe_3)_2\}]_2$ (5). Yield 62% (0.73 g, 0.93 mmol). Anal. Calcd for $C_{30}H_{76}N_8Si_4Zn_2$: C 45.49, H 9.67, N 14.15. Found: C 45.54, H 9.68, N 14.64. ^1H NMR (400.1 MHz, C_6D_6): δ 3.185 (q, J = 7.25 Hz, 16 H, N=C(N(*C*H_2CH_3)$_2$)$_2$), 1.026 (t, J = 7.02 Hz, 24 H, N=C(N(CH_2C*H*$_3$)$_2$)$_2$), 0.300 (s, 36 H N(Si(*C*H_3)$_3$)$_2$). ^{13}C NMR (100.6 MHz,C_6D_6):δ 164.7 (N=*C*(N-(CH_2CH_3)$_2$)$_2$), 44.2 (N=C(N(*C*H_2CH_3)$_2$)$_2$), 14.3(N=C(N(CH_2-*C*H_3)$_2$)$_2$), 6.1 (N(Si(*C*H_3)$_3$)$_2$). FT-IR (KBr, cm^{-1}) 2966 (s), 2894 (s), 1540 (s), 1516 (s), 1463 (s), 1378 (m), 1354 (m), 1254 (s), 1126 (m), 1073 (w), 1000 (s), 937 (w), 880 (s), 828 (s), 749 (w), 668 (m), 631 (w), 611 (w), 567 (w).

Synthesis of $[Mn(\mu\text{-OEt})(DBP)(H\text{-TEG})]_2$ (6). Compound **2** (0.63 g, 0.8 mmol) was dissolved in tetrahydrofuran (THF). In a separate vial ethanol 0.075 g (1.6 mmol) and H-DBP 0.34 g (1.6 mmol) were dissolved in THF. The solutions were mixed and left to stir for several hours. The solution was then concentrated via slow evaporation. Colorless crystals formed from solution at −35 °C in 24 h. Yield 39% (0.31 g, 0.3 mmol). Anal. Calcd for $C_{46}H_{84}Mn_2N_6O_4$: C 63.00, H 9.94, N 8.82. Found: C 62.51, H 9.75, 8.72. FT-IR (KBr, cm^{-1}) 3345 (w), 3051 (w), 2957 (s), 2859 (s), 1560 (s), 1500 (s), 1445 (s), 1410 (s), 1380 (s), 1363 (s), 1290 (s), 1260 (m), 1240 (s), 1200 (m), 1149 (w), 1126 (s), 1102 (s),

(11) Bunge, S. D.; Steele, J. L. *Inorg. Chem.* **2009**, *48*, 2701.
(12) Bunge, S. D.; Ocana, J. A.; Cleland, T. L.; Steele, J. L. *Inorg. Chem.* **2009**, *48*, 4619.
(13) Cleland, T. L.; Bunge, S. D. *Polyhedron* **2007**, *26*, 5506.
(14) Baster, D. V.; Chisholm, M. H.; Gama, G. J.; Hector, A. L.; Parkin, I. P. *Chem. Vap. Deposition* **1995**, *1*, 49. Dumestre, F.; Chaudret, B.; Amiens, C.; Renaud, P.; Fejes, P. *Science* **2004**, *303*, 821.
(15) Evans, D. F. *J. Chem. Soc.* **1959**, 2003. Schubert, E. M. *J. Chem. Educ.* **1992**, *69*, 62.

Scheme 1. (a) Synthesis of **1** and (b) the Zwitterionic Resonance of the TEG Anion

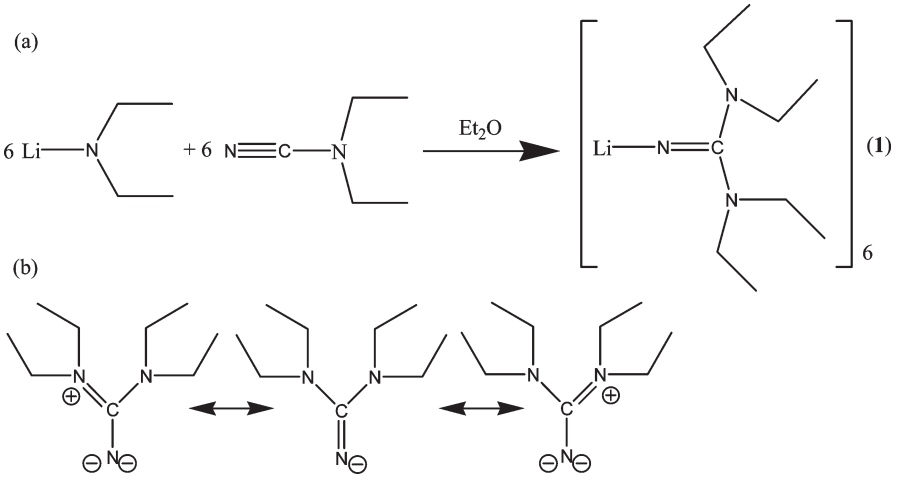

Scheme 2. General Synthesis of Complexes **2**−**5**

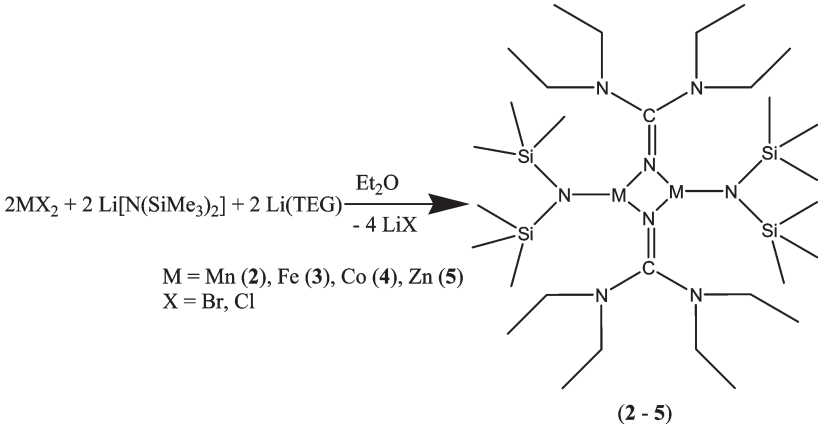

1057 (s), 889 (m), 869 (m), 820 (w), 786 (w), 749 (s), 715 (w), 651 (w), 542 (w), 487 (w), 451 (w). Magnetic moment (μ_B): 5.50.

X-ray Crystal Structure Information. X-ray crystallography was performed by mounting a crystal of **2**− **6** onto a thin glass fiber from a pool of Fluorolube and immediately placing it under a liquid N_2 cooled N_2 stream, on a Bruker AXS diffractometer. Crystals of **1** reacted vigorously with Fluorolube and thus a crystal was instead mounted from a pool of silicon oil. Lattice determination, data collection, structure refinement, scaling, and data reduction were carried out using the APEX2 version 1.0-22 software package.[16] Each structure was solved using direct methods. This procedure yielded the heavy atoms, along with a number of the N and C atoms. Subsequent Fourier synthesis yielded the remaining atom positions. The hydrogen atoms were fixed in positions of ideal geometry and refined within the XSHELL software.[17]

Results and Discussion

Synthesis. The convenient synthesis of lithium 1,1,3,3-tetramethylguanidinate via the reaction of lithium dimethylamide with dimethylcyanamide was first reported by Wade and co-workers.[7] Herein, we report the generalization of this reaction (Scheme 1) to generate $[Li(\mu\text{-TEG})]_6$ (**1**). Under an argon atmosphere, to a hexanes solution of lithium diethylamide, 1 equiv of a diethylcyanamide is added. The solution is then heated to reflux and stirred for 10 min. Colorless crystals of **1** are isolated in 78% yield from a concentrated hexanes solution at −35 °C. The reactivity of **1** precluded obtaining satisfactory elemental analysis. Li(TEG) was therefore generated *in situ* for described reactions.

Li(TEG) was subsequently used in conjunction with $LiN(SiMe_3)_2$ and MX_2 (MX_2 = $MnBr_2$, $FeBr_2$, $CoBr_2$, and $ZnCl_2$) to form the corresponding heteroligated M-(TEG) complex, $[M(\mu\text{-TEG})\{N(SiMe_3)_2\}]_2$ (**2**−**5**). The synthesis of compounds **2**−**5** is shown in Scheme 2. The reactions are performed in ether. In each synthesis, the ether is removed under vacuum, and hexanes is added. The insoluble precipitate is removed from solution via centrifugation. The reaction mixture is then concentrated and cooled to −35 °C to facilitate crystallization. All four complexes were isolated as crystals in yields from 25 to 62%. For elemental analysis, recrystallization was additionally performed by redissolving the isolated solid in hexanes and then cooling the sample to −35 °C for 24 h. Dried crystals of **2**−**5** are stable under argon at −35 °C for several months.

The synthesis of compound **6** is depicted in Scheme 3. The intent of this synthesis is to examine the reactivity of **2** through the possible isolation of a complex isostructural to the previously reported 1,1,3,3-tetramethylguanidine (H-TMG) solvated $[M(\mu\text{-OEt})(DBP)(H\text{-TMG})]_2$

(16) *APEX2*, version 1.0-22; Bruker AXS, Inc.: Madison, WI, 2005.
(17) Sheldrick, G. M. *Acta Crystallogr., Sect. A* **2008**, *64*, 112.

Scheme 3. Synthesis of Complex **6**

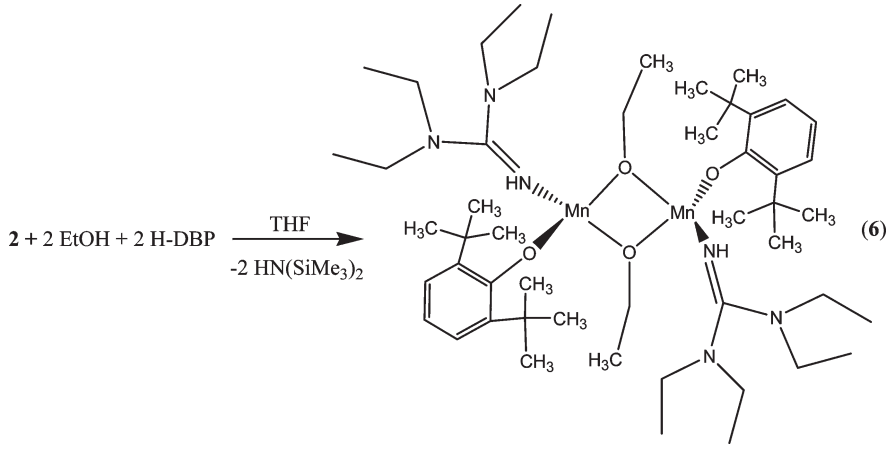

(M = Zn and Mg).[10,18] The alcoholysis of metal amides is typically a straightforward route for isolating alkali-metal-free transition metal alkoxides.[19] In a THF solution, 1 equiv of **2** was reacted with 2 equiv of ethanol and 2 equiv of H-DBP. The solution was stirred for 2 h, concentrated, and then cooled to −35 °C for 24 h to generate colorless crystals of **6** (39% yield).

Structural Descriptions. All six complexes were characterized by X-ray crystallography. Thermal ellipsoid plots of **1**, **2**, and **6A** are shown in Figures 1−3. The data collection parameters are presented in Tables 1 and 2, and selected interatomic distances and angles are provided in Figures 1−3 and in Table 3. Structural descriptions for the complexes are provided in the following paragraphs. Because of the similarity, when appropriate, a general description for complexes **2**−**5** is provided.

[Li(*μ*-TEG)]$_6$ (1). Complex **1** (Figure 1) belongs to the same structural family as the hexanuclear lithium complexes: [Li{μ-N=C(^{t}Bu)(Ph)}]$_6$, [Li{μ-N=C(NMe$_2$)(Ph)}]$_6$, and [Li{μ-N=C(NMe$_2$)$_2$}]$_6$.[6,7,20] **1** crystallized in the cubic space group, $Pn\bar{3}$, with four molecules per unit cell. Each cluster contains a puckered chair-shaped Li$_6$ ring with six TEG ligands triply bridging to six triangular Li$_3$ faces. The bridging imino nitrogen atoms are roughly equidistant from the three lithium atoms, with the mean Li−N distance being 2.02 Å. The C=N$_{imino}$ donor of the TEG ligand falls within the range of a carbon−nitrogen double bond (1.262 Å). The other two C−N distances (1.4247(14) Å and 1.4507(13) Å) are consistent for C−N single bonds.

[M(*μ*-TEG){N(SiMe$_3$)$_2$}]$_2$ (2−5). The structures of **2**−**5** exhibit only minor variation with alteration of the metal and are represented by the thermal ellipsoid plot of **2** shown in Figure 2. Each complex crystallizes in the triclinic space group $P\bar{1}$ with two molecules per unit cell. The molecular structures consist of a dinuclear unit with a square M$_2$N$_2$ ring. Each metal atom is coordinated to one terminal amido ligand and is linked to the other metal atom by two symmetrical bridging imino groups. The M−N−M angle ranged from 82.28° to 91.61°. The C=N$_{imino}$ donor distance of the TEG ligand ranges from 1.262 Å to 1.296 Å and these are typical for a carbon−nitrogen double bond. The other two C−N distances range from 1.382 Å to 1.407 Å, and the interactions of these N atoms with metals are negligible (the shortest M···N distance is ∼3.5 Å). There is an additional angle ranging from 39.35° to 58.79° between the plane of the "CN $_3$" framework of the TEG group and the plane of the square M$_2$N$_2$ unit. The two silicon atoms on each disilylamide reside on opposite sides of the M$_2$N$_2$ plane.

Low-coordinate d-block amides are relatively rare.[13,21−32] To place the family of TEG complexes into context, Table 5 lists the interatomic M−N distances, N−M−N angles, and M···M distances for previously reported low-coordinate dinuclear Mn, Fe, Co, and Zn amides and imides. Complexes **2**−**5** are perhaps best compared to the corresponding bis(trimethylsilyl)amides, [M{μ-N(SiMe$_3$)$_2$}{N(SiMe$_3$)$_2$}]$_2$.[21,22,24] The replacement of two disilylamides by two TEG ligands results in a slight decrease in the average M−N distance and a corresponding decrease in the M···M separation. The distances for **2**−**5** are quite short in comparison to other *d*-block dinuclear units and are clearly enforced by the TEG ligand geometry.

[Mn(*μ*-OEt)(DBP)(H-TMG)]$_2$ (6). Compound **6** crystallized in the monoclinic space group *C*2/*c* with two crystallographically inequivalent (**6A** and **6B**) but

(18) Monegan, J. D.; Bunge, S. D. *Inorg. Chem.* **2009**, *48*, 3248.
(19) Bradley, D. C.; Mehrotra, R. C.; Rothwell, I. P.; Singh, A. *Alkoxo and Aryloxo Derivatives of Metals*; Elsevier: New York, 2001.
(20) Clegg, W.; Snaith, R.; Shearer, H. M. M.; Wade, K.; Whitehead, G. *J. Chem. Soc., Dalton Trans.* **1983**, 1309.
(21) Murray, B. D.; Power, P. P. *Inorg. Chem.* **1984**, *23*, 4584.
(22) Bradley, D. C.; Hursthouse, M. B.; Malik, K. M. A.; Moseler, R. *Transition Met.Chem.* **1978**, *3*, 253.
(23) Belforte, A.; Calderazzo, F.; Englert, U.; Straehle, J.; Wurst, K. *J. Chem. Soc., Dalton Trans.* **1991**, 2419.
(24) Olmstead, M. M.; Power, P. P.; Shoner, S. C. *Inorg. Chem.* **1991**, *30*, 2547.
(25) Koster, R.; Seidel, G.; Boese, R.; Wrackmeyer, B. *Chem. Ber.-Rec.* **1987**, *120*, 669.
(26) Hope, H.; Olmstead, M. M.; Murray, B. D.; Power, P. P. *J. Am. Chem. Soc.* **1985**, *107*, 712.
(27) Krieger, M.; Gould, R. O.; Neumuller, B.; Harms, K.; Dehnicke, K. *Z. Anorg. Allg. Chem.* **1998**, *624*, 1434.
(28) Schumann, H.; Gottfriedsen, J.; Girgsdies, F. *Z. Anorg. Allg. Chem.* **1997**, *623*, 1881.
(29) Armstrong, D. R.; Forbes, G. C.; Mulvey, R. E.; Clegg, W.; Tooke, D. M. *J. Chem. Soc., Dalton Trans.* **2002**, 1656.
(30) Putzer, M. A.; Dashti-Mommertz, A.; Neumuller, B.; Dehnicke, K. *Z. Anorg. Allg. Chem.* **1998**, *624*, 263.
(31) Just, O.; Gaul, D. A.; Rees, W. S. *Polyhedron* **2001**, *20*, 815.
(32) Schumann, H.; Gottfriedsen, J.; Dechert, S.; Girgsdies, F. *Z. Anorg. Allg. Chem.* **2000**, *626*, 747.

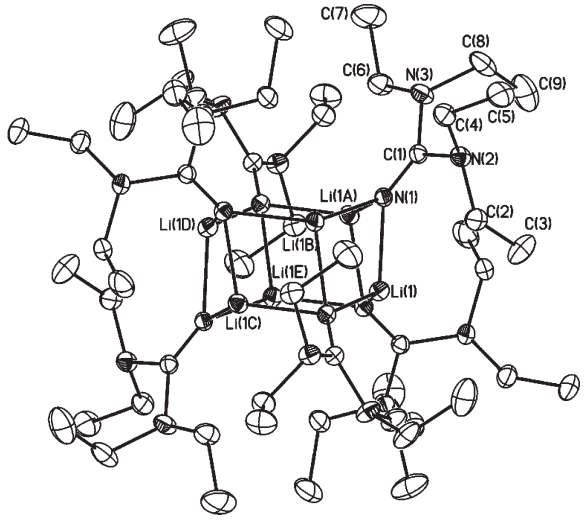

Figure 1. Thermal ellipsoid plot of **1**. Ellipsoids are drawn at the 30% level. Selected interatomic distances (Å) and angles (deg): Li(1)−N(1) 1.996(2), Li(1)−N(1A) 2.026(2), Li(1)−N(1B) 2.037(2), N(1)−C(1) 1.2554(14), N(2)−C(1) 1.4247(14), N(3)−C(1) 1.4507(13); N(1)−Li(1)−N(1A) 104.19(9), N(1)−Li(1)−N(1B) 128.48(11), N(1A)−Li(1)−N(1B) 102.72(9).

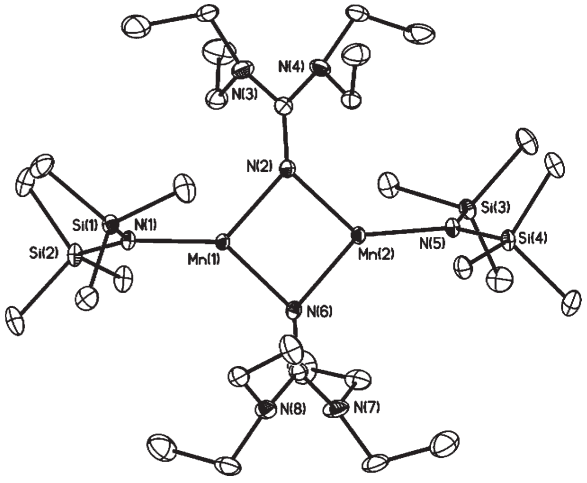

Figure 2. Thermal ellipsoid plot of **2**. Ellipsoids are drawn at the 30% level. Selected interatomic distances (Å) and angles (deg): Mn(1)−N(1) 2.011(2), Mn(1)−N(2) 2.028(2), Mn(1)−N(6) 2.052(2), N(2)−C(22) 1.287(4), N(3)−C(22) 1.383(4), N(4)−C(22) 1.394(4), Si(1)−N(1) 1.7064(19); Mn(2)−N(2)−Mn(1) 89.36(9), N(2)−Mn(1)−N(6) 91.28(9), Si(3)−N(5)−Si(4) 127.70(13).

structurally similar complexes per unit cell. **6A** and **6B** are illustrated in Figures 3 and Supporting Information, Figure S4, respectively. There are significant differences in the orientation of the terminal DBP and H-TEG ligands in **6A** and **6B**, but the same gross structural features are found in both molecules. Each molecule contains a planar Mn_2O_2 core with a distorted tetrahedral Mn atom connected to an adjacent manganese by two bridging ethoxide ligands. The Mn···Mn distances are ~3.1 Å for both molecules. The tetrahedral coordination is fulfilled through additional coordination of the Mn to one terminal DBP and one terminal H-TEG. In both complexes, the Mn−O distances fall within the expected ranges of 1.955 Å to 2.055 Å, while the terminal Mn−N distances are 2.14 Å. A notable feature of both **6A** and **6B** are the terminal Mn−O−Ar angles of ~168°. This is a

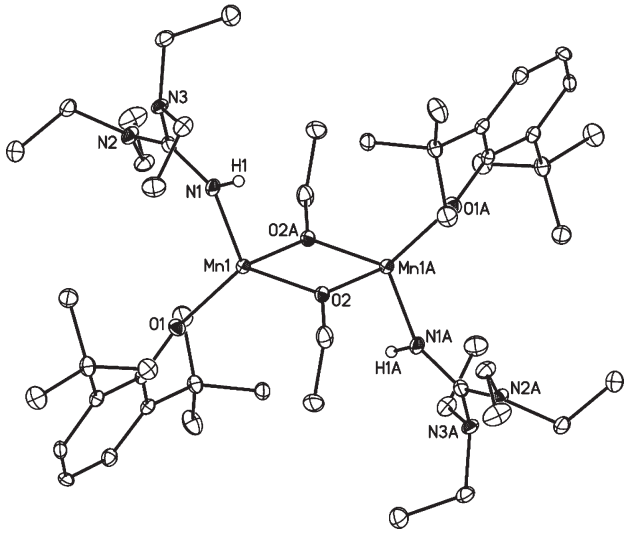

Figure 3. Thermal ellipsoid plot of **6A.** Ellipsoids are drawn at the 30% level. Selected interatomic distances (Å) and angles (deg): Mn(1)−O(1) 1.955(3), Mn(1)−O(2) 2.056(3), Mn(1)−N(1) 2.126(4), N(1)−C(17) 1.320(6); Mn(1)−O(2)−Mn(1A) 98.17(13), O(1)−Mn(1)−N(1) 112.39(14), O(1)−Mn(1)−O(2) 118.09(13), C(1)−O(1)−Mn(1) 167.3(3).

Table 1. Data Collection Parameters for **1**−**3**

	1	**2**	**3**
chemical formula	$C_{54}H_{120}Li_6N_{18}$	$C_{30}H_{76}Mn_2N_8Si_4$	$C_{30}H_{76}Fe_2N_8Si_4$
formula weight	1063.32	771.23	773.05
temp (K)	100(2)	100(2)	100(2)
space group	cubic	triclinic	triclinic
	$Pn\bar{3}$	$P\bar{1}$	$P\bar{1}$
a (Å)	19.0172(6)	11.5092(14)	8.8516(5)
b (Å)		13.6191(16)	12.5142(7)
c (Å)		15.8877(19)	21.0375(11)
α (deg)		73.881(2)	87.1550(10
β (deg)		87.565(2)	80.3400(10)
γ (deg)		69.869(2)	75.6160(10)
V (Å^3)	6877.6(4)	2242.4(5)	2225.2(2)
Z	4	2	2
D_{calcd}(Mg/m^3)	1.027	1.142	1.154
μ,(Mo, Kα) (mm^{-1})	0.062	0.698	0.788
R1[a] (%) (all data)	4.31(6.03)	4.05 (5.24)	4.43 (5.52)
wR2[b] (%)(all data)	11.03(12.68)	12.82 (14.25)	14.85 (15.92)

[a] $R1 = \sum||F_o| - |F_c||/\sum|F_o| \times 100$. [b] $wR2 = [\sum w(F_o^2 - F_c^2)^2/\sum w(F_o^2)^2]^{1/2} \times 100$.

larger angle than the structurally similar dinuclear zinc complex $[Zn(\mu\text{-OEt})(H\text{-TMG})\{OC_6H_3(CMe_3)_2\text{-}2,6\}]_2$.[10] Early and mid-transition metal aryloxide compounds typically possess larger M−O−Ar angles because of the potential π-donation from the aryl ring to the metal center.

The major differences between **6A** and **6B** involve the orientations that the terminal guanidine and aryloxide have with respect to each other and to that of the Mn_2O_2 plane. In **6A**, the N−Mn−OAr angle is significantly larger (112.40°) versus that found in **6B** (95.39°). Because of similarities in Mn−O−Ar angles in both molecules, the difference in N−Mn−OAr angle generates a decrease in the angle between the plane of the "OAr" framework and the plane of the M_2O_2 unit {70.18° (**6A**); 36.64° (**6B**)}. This consequently results in an additional disparity between the plane of the "CN_3" framework of the H-TEG and the plane of the M_2O_2 unit, 62.25° for **6A** and 89.39° for **6B**.

Table 2. Data collection parameters for **4**−**6**

	4	**5**	**6**
chemical formula	$C_{30}H_{76}Co_2N_8Si_4$	$C_{30}H_{76}N_8Si_4Zn_2$	$C_{50}H_{94}Mn_2N_6O_4$
formula weight	779.21	792.09	953.19
temp (K)	100(2)	100(2)	100(2)
space group	triclinic $P\bar{1}$	triclinic $P\bar{1}$	monoclinic $C2/c$
a (Å)	9.0193(17)	9.1375(10)	52.119(7)
b (Å)	12.383(2)	12.6756(18)	9.8361(12)
c (Å)	21.445(4)	21.716(3)	21.134(3)
α (deg)	89.757(3)	84.845(10)	
β (deg)	84.648(3)	84.596(7)	95.398(5)
γ (deg)	69.069(3)	69.073(7)	
V (Å^3)	2226.1(7)	2334.6(5)	10786(2)
Z	2	2	8
D_{calcd}(Mg/m^3)	1.162	1.127	1.174
μ,(Mo, Kα) (mm^{-1})	0.881	1.157	0.513
R1[a] (%) (all data)	2.96 (3.78)	4.96 (8.69)	6.83 (12.42)
wR2[b] (%) (all data)	9.71 (10.55)	13.41 (16.12)	18.03 (20.89)

[a] $R1 = \sum||F_o| - |F_c||/\sum|F_o| \times 100$. [b] $wR2 = [\sum w(F_o^2 - F_c^2)^2/\sum w(F_o^2)^2]^{1/2} \times 100$.

Spectroscopic Studies and Magnetic Data. Crystals of **1**−**6** were dried *in vacuo* to yield the bulk powder and used subsequently in the following analyses. All complexes are readily soluble in toluene, and both **1** and **5** exhibited expected ^{1}H and ^{13}C resonances in the solution NMR spectra. In the ^{1}H NMR spectra, the $N(SiMe_3)_2$ ligand for **5** is implied by the observation of a singlet at $\delta = 0.30$. For **1** and **5**, the expected resonances for ethyl substituents of the guanidinate ligand are additionally present. In the ^{13}C NMR spectra, the low field resonance (∼160 ppm) for the central carbon atom "CN_3" of the TEG ligand is an additional distinguishing feature.

For **1**−**6**, FT-IR spectroscopy was utilized to confirm the υ(C=N) of the absorptions bands around 1550 cm^{-1} corresponding to the N_{imino} donor coordinated to the metal. This is lower than that found in $HN=C(NMe_2)_2$, 1600 cm^{-1}. A good comparison can be found in the 1512 cm^{-1} stretching frequency attributed to the imino group in $[\{Sn(\eta^3\text{-}C_5H_5)\text{-}[\mu\text{-}N{=}C(NMe_2)_2]\}_2]$.[8] In **6**, the presence of υ(N−H) was confirmed by stretching corresponding to a peak around 3345 cm^{-1}. Assignment of the Mn−O bands in alkoxides and aryloxides is frequently difficult owing to the coupling of the C−O and Mn−O modes. Comparisons of the data for **6** with data for H-DBP and **2** indicate that, in the case of **6**, bands located between 540 and 450 cm^{-1} are most likely associated with the Mn−O bonds.

The UV−vis absorption spectra of compounds **2**−**4** were obtained in hexanes solution and are characterized by intense absorptions at wavelengths shorter than 390 nm that are attributable to π−π* transitions of the metal-to-TEG charge transfer transitions. For **2** and **3**, the intense peaks trail into the visible region and are consistent with the appearance of pink and yellow colors for these complexes. Consistent with previously reported low-coordinate Co(II) amides, the intensely colored (dark blue/black) **4** features two prominent absorptions (ε values greater than 13800) in the visible region (504 and 688 nm).

The magnetic moments of compounds **2**−**4** and **6** were determined at room temperature in toluene/deuterated toluene by the Evans method. These values are presented in Table 5. A high-spin configuration is expected for **2**−**4** in view of the three-coordinate geometry of the metals that gives rise to a relatively weak ligand field. However, the values for the magnetic moments are considerably less than the spin-only values, indicating that there is significant antiferromagnetic coupling between metal atoms. In comparison, because of the considerably longer Mn···Mn separation (3.1 Å), the magnetic moment of **6** (5.50 μ_B) is consistent with a spin-only 5/2 value for each tetrahedral Mn with little indication of coupling between metal centers.

Table 3. Selected Inter-Atomic Distances (Å) and Angles (deg) for **3**−**5**

Complex 3			
N(1)−Fe(1)	1.952(2)	N(1)−Fe(2)	1.956(2)
N(4)−Fe(1)	1.957(3)	N(4)−Fe(2)	1.963(2)
N(8)−Fe(1)	1.930(2)	N(7)−Fe(2)	1.928(2)
C(10)−N(4)	1.298(4)	C(1)−N(1)	1.296(4)
C(10)−N(5)	1.403(4)	C(1)−N(2)	1.401(4)
C(10)−N(6)	1.377(4)	C(1)−N(3)	1.369(4)
N(8)−Fe(1)−N(1)	131.79(10)	N(7)−Fe(2)−N(1)	131.84(10)
N(8)−Fe(1)−N(4)	132.62(10)	N(7)−Fe(2)−N(4)	132.91(10)
N(1)−Fe(1)−N(4)	95.59(10)	N(1)−Fe(2)−N(4)	95.25(10)
Fe(1)−N(1)−Fe(2)	84.70(10)	Fe(1)−N(4)−Fe(2)	84.38(10)
Si(3)−N(8)−Fe(1)	115.72(14)	Si(1)−N(7)−Fe(2)	116.91(13)
Si(4)−N(8)−Fe(1)	118.09(14)	Si(2)−N(7)−Fe(2)	118.66(13)
Si(4)−N(8)−Si(3)	126.19(15)	Si(2)−N(7)−Si(1)	124.40(15)
Complex 4			
Co(1)−N(1)	1.9342(15)	Co(2)−N(1)	1.9478(15)
Co(1)−N(2)	1.9389(15)	Co(2)−N(2)	1.9442(15)
Co(1)−N(4)	1.9030(15)	Co(2)−N(3)	1.9108(15)
N(2)−C(2)	1.287(2)	N(1)−C(1)	1.285(2)
C(2)−N(7)	1.394(2)	C(1)−N(5)	1.389(2)
C(2)−N(8)	1.392(2)	C(1)−N(6)	1.407(2)
N(4)−Co(1)−N(1)	133.47(6)	Co(1)−N(2)−Co(2)	82.25(6)
N(4)−Co(1)−N(2)	128.07(6)	N(3)−Co(2)−N(1)	130.79(6)
N(1)−Co(1)−N(2)	97.58(6)	N(3)−Co(2)−N(2)	132.08(6)
Si(1)−N(4)−Co(1)	113.55(8)	N(2)−Co(2)−N(1)	96.95(6)
Si(2)−N(4)−Co(1)	115.76(8)	Si(3)−N(3)−Co(2)	115.30(8)
Si(2)−N(4)−Si(1)	130.67(9)	Si(4)−N(3)−Co(2)	117.12(9)
Co(1)−N(1)−Co(2)	82.28(6)	Si(3)−N(3)−Si(4)	127.46(9)
Complex 5			
Zn(1)−N(1)	1.982(4)	Zn(2)−N(1)	1.966(3)
Zn(1)−N(2)	1.954(3)	Zn(2)−N(2)	1.971(4)
Zn(1)−N(7)	1.897(3)	Zn(2)−N(8)	1.898(3)
N(2)−C(1)	1.266(6)	N(4)−C(1)	1.397(7)
N(3)−C(1)	1.386(6)		
N(7)−Zn(1)−N(1)	137.19(15)	N(8)−Zn(2)−N(1)	134.48(15)
N(7)−Zn(1)−N(2)	134.42(16)	N(8)−Zn(2)−N(2)	136.96(15)
N(2)−Zn(1)−N(1)	88.14(14)	N(1)−Zn(2)−N(2)	88.10(14)
Si(1)−N(7)−Zn(1)	117.6(2)	Si(3)−N(8)−Zn(2)	113.96(19)
Si(2)−N(7)−Zn(1)	115.6(2)	Si(4)−N(8)−Zn(2)	116.6(2)
Si(2)−N(7)−Si(1)	126.8(2)	Si(4)−N(8)−Si(3)	129.4(2)

Resonance of the TEG Ligand. The zwitterionic resonance structure of the TEG anion facilitates delocalization of the negative charge on the N_{imino} atom (See Scheme 1). A method to assess the degree of delocalization within the "−N=C−N−" component of the TEG ligand is the Δ_{CN} parameter; $\Delta_{CN} = d(C-N) - d(C=N)$. [33] Δ_{CN} values range from 0 Å in a fully delocalized system and up to ∼0.10 Å in a fully localized system. For complexes **2**− **5**, the average value of Δ_{CN} can be calculated from the crystallographic data (0.134 Å, Mn; 0.092 Å, Fe; 0.111 Å, Co; 0.135 Å, Zn). Care must be taken in over interpret-

(33) *The Chemistry of Functional Groups: the Chemistry of Amidines and Imidates*; Patai, S., Ed.; Wiley: New York, 1975.

Table 4. Structurally Characterized $[M(\mu\text{-}NR)(NR_2)]_2$ Complexes

complex	M−*N* (Å)	M···M (Å)	M−*N*−M (deg)	ref.
Mn				
$[Mn\{\mu\text{-}\{N(SiMe_3)_2\}\}\{N(SiMe_3)_2\}]$	2.17	2.81	80.62	21,22
$[Mn\{\mu\text{-}(N\textit{i}\text{-}Pr_2)(N\textit{i}\text{-}Pr_2)]$	2.14	2.84	83.35	23
$[Mn(\mu\text{-TEG})\{N(SiMe_3)_2\}]$ (**2**)	2.03	2.85	87.97	*
Fe				
$[Fe(\mu\text{-TEG})\{N(SiMe_3)_2\}]$ (**3**)	1.95	2.63	84.70	*
$[Fe\{\mu\text{-}\{N(SiMe_3)_2\}\}\{N(SiMe_3)_2\}]$	2.08	2.66	79.41	24
$[Fe\{\mu\text{-}NB(Et)_2C(Et)C(CH_3)Si(CH_3)_2\}\{NB(Et)_2C(Et)C(CH_3)Si(CH_3)_2\}]$	2.04	2.69	82.42	25
$[Fe\{\mu\text{-}(NPh_2)(NPh_2)]$	2.04	2.72	83.56	24
Co				
$[Co(\mu\text{-TEG})\{N(SiMe_3)_2\}]$ (**4**)	1.94	2.55	82.28	*
$[Co\{\mu\text{-}\{N(SiMe_3)_2\}\}\{N(SiMe_3)_2\}]$	2.06	2.58	77.59	21
$[Co(\mu\text{-}(NPh_2)(NPh_2)]$	2.00	2.57	79.86	26
Zn				
$[Zn\{\mu\text{-}(N{=}PEt_3)\}\{N(SiMe_3)_2\}]$	1.95	2.77	90.53	27
$[Zn\{\mu\text{-}\{N(\textit{i}\text{-}Bu)_2\}\{N(\textit{i}\text{-}Bu)_2\}]$	2.03	2.78	86.63	28
$[Zn\{\mu\text{-}\{N(CH_2Ph)_2\}\{N(CH_2Ph)_2\}]$	2.04	2.80	86.88	29
$[Zn\{\mu\text{-}(N{=}C(NEt_2)(NCH_2CH_2CH_2CH_2)\}\{N(SiMe_3)_2\}]$	1.96	2.80	90.77	13
$[Zn\{\mu\text{-}(N{=}C(NCH_2CH_2CH_2CH_2)_2\}\{N(SiMe_3)_2\}]$	1.95	2.80	91.50	13
$[Zn(\mu\text{-TEG})\{N(SiMe_3)_2\}]$ (**5**)	1.97	2.82	91.61	*
$[Zn\{\mu\text{-}(NPh_2)\}(NPh_2)]$	2.03	2.83	88.14	30
$[Zn\{\mu\text{-}(N{=}C(N\,CH_2CH_2\,CH_2CH_2CH_2)(NEt_2)\}\{N(SiMe_3)_2\}]$	1.97	2.83	91.69	13
$[Zn\{\mu\text{-}(N{=}C(NMe_2)(N\,CH_2CH_2CH_2CH_2)\}\{N(SiMe_3)_2\}]$	1.96	2.84	92.47	13
$[Zn\{\mu\text{-}NSi(CH_3)_2\,CH_2CH_2Si(CH_3)_2\}\{NSi(CH_3)_2CH_2CH_2Si(CH_3)_2\}]$	2.06	2.86	88.08	31
$[Zn\{\mu\text{-}N(Ph)(SiMe_3)\}\{N(Ph)(SiMe_3)_2\}]$	2.05	2.87	88.74	32

* This work

Table 5. Magnetic Moment (298 K, μ_B) and UV-vis Absorption Data λ_{max} (nm) for **2**−**4** and **6** with ε (mL mol^{-1} cm^{-1}) Values in Parentheses

complex	magnetic moment	UV−vis abs. data
$[Mn(\mu\text{-TEG})\{N(SiMe_3)_2\}]$ (**2**)	4.30	328 (36700)
$[Fe(\mu\text{-TEG})\{N(SiMe_3)_2\}]$ (**3**)	2.77	301 (128000), 388 (14800), 456 (6710)
$[Co(\mu\text{-TEG})\{N(SiMe_3)_2\}]$ (**4**)	3.35	279 (288000), 504 (28500), 688 (13900)
$[Mn(\mu\text{-OEt})(DBP)(H\text{-TMG})]_2$ (**6**)	5.50	

ing the data. For complexes **2**−**5**, the Δ_{CN} corresponds to a localized system with each TEG retaining unperturbed C−N and C=N groups. These are similar to Δ_{CN} values calculated for recently reported tetranuclear $[M_2(\mu\text{-TAG})\{\mu\text{-}N(SiMe_3)_2\}]$ (M = Cu, Ag, and Au) complexes.[11]

Concluding Remarks

In this work, the following conclusions can be garnered: (i) the addition of lithium diethylamide to diethylcyanamide provides a convenient route for the synthesis of lithium tetraethylguanidinate, **1**; (ii) reaction of **1** and $LiN(SiMe_3)_2$with Mn^{II}, Fe^{II}, Co^{II}, and Zn^{II} halides results in metathetical exchange and the formation of dinuclear guanidinates, **2**−**5**; (iii) structural examination of **2**− **5** indicates that TEG has a tendency to bridge between the metals and facilitates the isolation of crystalline solids that are dinuclear in solution; and (iv) the reaction of **2** with sterically varied alcohols results in protonation and subsequent liberation of $HN(SiMe_3)_2$, retention of a coordinated H-TEG, and the isolation of a rare example of a well-defined dinuclear Mn^{II} ethoxide.

From a broader perspective, it is noteworthy that complexes **2**−**5** are synthesized in moderate yield, are free of lithium halide contaminant, and contain relatively short M···M separations. Such features are advantageous if these compounds are to be further reacted with protic reagents and/or used in material syntheses. On the basis of the success in synthesizing **6**, additional syntheses with **2**−**5** are currently under way. Along with this effort, our investigations are aimed at further examining the steric and electronic features of the TAG ligand-set that influence coordination, nuclearity, and reactivity.

Acknowledgment. The authors acknowledge Kent State University and the National Science Foundation (NSF-REU) for support of this work.

Supporting Information Available: The plots for **3**, **4**, **5**, and **6B** are found in Figures S1−S4. This material is available free of charge via the Internet at http://pubs.acs.org. Crystallographic data (excluding structure factors) for the structures have been deposited with the Cambridge Crystallographic Data Centre as supplementary publication nos. CCDC 722744 for **1**, CCDC 722745 for **2**, CCDC 722746 for **3**, CCDC 722747 for **4**, CCDC 722748 for **5**, and CCDC 722749 for **6**. Copies of the data can be obtained on application to CCDC, 12 Union Road, Cambridge CB2 1EZ, UK (fax, +44-(0)1223−336033; or e-mail, deposit@ccdc.cam.ac.uk).